Joint Pathology Center
Veterinary Pathology Services

WEDNESDAY SLIDE CONFERENCE 2013-2014

Conference 6

23 October 2013

CASE I: WSC 2013, Case #2 (4032579).

Signalment: 6-month-old female Nubian goat, (*Capra hircus*).

History: This goat belonged to a small (<20) flock of sheep and goats at a newly developed community supported agriculture farm. Animals were acquired from multiple sources. This goat had a two-week history of respiratory tract infection, corneal edema, blindness and weakness of the hind end. The animal was euthanized.

Gross Pathology: The goat was in poor body condition. There was cloudiness of the cornea of each eye. Approximately 70 % of the cranioventral regions of the lungs were dark red and consolidated, and there was abundant white froth in the lumen of the trachea. Multiple segments of the small intestine had a reddened

1-1. Kidney, goat: Renal vessels of various sizes are surrounded by a dense cellular infiltrate. (HE 0.63X)

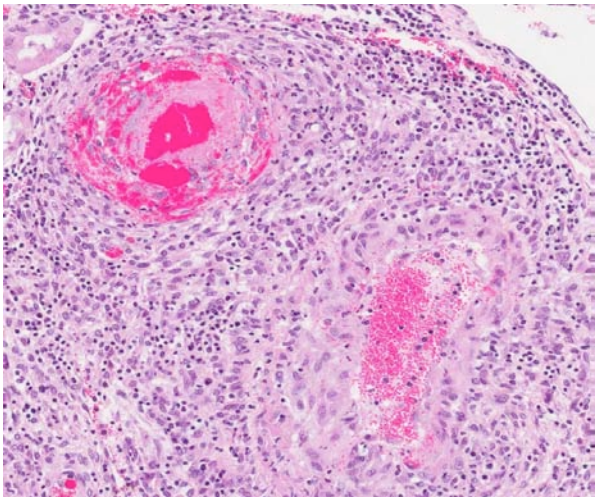

1-2. Kidney, goat: Brightly eosinophilic protein, hemorrhage, and cellular debris expands the wall of the arteriole at upper left (fibrinoid necrosis), the wall of both vessels is further expanded by disorganized smooth muscle, fibroblasts, and infiltrating lymphocytes. (HE 64X)

serosa. There were multiple, pinpoint, white foci on the liver surface and throughout the parenchyma. White pulp was prominent on the cut surface of the spleen. The mesenteric and sublumbar lymph nodes were moderately enlarged.

Laboratory Results: Capnophilic [10 %] culture of the lung yielded *Mycoplasma* sp. There was no bacterial growth on capnophilic [10 %] culture of the liver. A sample of kidney was submitted to the National Veterinary Services Laboratory, Ames, IA for testing by nested polymerase chain reaction (PCR) for the presence of alcelaphine herpesvirus 1 (AlHV-1) and ovine herpesvirus 2 (OvHV-2) DNA. OvHV-2 DNA was detected in the sample.

Histopathologic Description: Kidney: Affecting multiple blood vessels, predominantly arteries, in the cortex, corticomedullary junction (including arcuate and interlobular arteries) and pelvis, there is necrotizing vasculitis, characterized by marked expansion and disruption of one to all tunicae of vessel walls by an infiltrate composed of large numbers of lymphocytes together with lesser numbers of macrophages and lymphoblasts, and occasional plasma cells. These infiltrates often involve the outer margin of the media and the adventitia, and markedly expand the perivascular interstitium, occasionally surrounding glomeruli or tubules. In the tunica media of some affected arteries, the cellular infiltrate is admixed with homogeneous to fibrillar to beaded eosinophilic material, and pyknotic and karyorrhectic debris. There is disruption of the intima and/or hypertrophy of endothelium in affected vessels; rare fibrin thrombi partially occlude the lumen of several vessels (variation among the slides). Multifocally in the cortex, there is infiltration by low to medium numbers of lymphocytes, lesser numbers of macrophages and plasma cells in the interstitium. There is a small proportion of tubules that are moderately ectatic and contain aggregates of degenerate cells and necrotic cellular debris in the lumen or are lined by epithelial cells that contain cytoplasmic eosinophilic droplets. A loosely organized infiltrate of low to medium numbers of lymphocytes is present subjacent to the urothelium of the pelvis (variation among slides). There is moderate congestion, and occasional small hemorrhages in some areas.

Contributor's Morphologic Diagnosis: Kidney: Severe, multifocal, lymphohistiocytic and lymphoblastic, chronic necrotizing vasculitis and perivasculitis with mild multifocal lymphocytic interstitial nephritis, tubular degeneration and necrosis.

Contributor's Comment: This case is a rare example of malignant catarrhal fever (MCF) in a goat, which highlights the susceptibility of goats to clinical disease from OvHV-2 infection, albeit very uncommon.

Malignant catarrhal fever is a herpesviral disease with a worldwide distribution that affects certain wild and domestic species of the order *Artiodactyla*.[2] It is caused by closely related viruses in the genus *Macavirus* (sigla for malignant catarrhal fever virus) in the subfamily Gammaherpesvirinae.[4] The International Committee on Taxonomy of Viruses (ICTV) currently recognizes 9 species in the genus,[7] of which probably the best known are alcelaphine herpesvirus 1 and ovine herpesvirus.[2] Gammaherpesviruses have a propensity to become latent. As a result, the gammaherpesviruses have co-evolved with their natural hosts. Unless natural hosts are immunodeficient, gammaherpesviruses are normally carried asymptomatically. However, natural hosts act as reservoirs and are sources of infection to susceptible cloven-hoofed species that are not as highly adapted to the virus.[1]

Molecular phylogenetic analysis of a portion of the DNA polymerase gene that is relatively conserved among herpesviruses has revealed two major groups of MCF viruses. This is relevant not only because viruses within each group have similar biological properties, but also because it is suggestive of a shared epidemiology.[8] Most MCF viruses are named after their reservoir hosts, and the two aforementioned groups are the following (note: this analysis included viruses not yet classified by the ICTV):[7]

The alcelaphinae/hippotragine group, which includes AIHV-1, the virus responsible for wildebeest-associated MCF; alcelaphine herpesvirus 2 (AIHV-2), hippotragine herpesvirus 1 (HiHV-1) and MCF virus oryx (MCFV-oryx) which are carried asymptomatically by hartebeest, roan antelope and oryx, respectively, have not yet been associated with disease.[8]

The caprine group, which includes MCF virus-white tailed deer (MCFV-WTD) of unknown origin that causes disease in white-tailed deer; MCF virus carried by ibex (MCFV-ibex), which is responsible for disease in bongo antelope and anoa; MCF virus in muskox (MCFV-muskox) and aoudad (MCF-aoudad), which are carried asymptomatically and have not yet been associated with disease; caprine herpesvirus 2 (CpHV-2) which is endemic in goats and has been associated with disease in sika deer, white-tailed deer and pronghorn antelopes; and OvHV-2.[8]

OvHV-2 is one of the most characterized causative agents of MCF. The virus is endemic in most domesticated sheep.[8,11] MCF-like disease has been experimentally induced in sheep by aerosol inoculation with high doses of OvHV-2; however, the disease is uncommon or non-existent under natural conditions.[10] The susceptibility of ruminant species to development of MCF varies significantly. Père David's deer, banteng (aka Bali cattle), and bison are most susceptible to disease, followed by water buffalo. Domestic cattle (*Bos taurus* and *Bos indicus*) are comparatively resistant; for example, bison are 1000 times more susceptible to clinical MCF than cattle. The reason for this range in susceptibility is not known. Sheep-associated MCF has occasionally been reported in moose and pigs.[13]

There are few reports of sheep-associated MCF in domestic goats in Europe (Germany and United Kingdom). In two published cases, the most common clinical presentation included pyrexia and neurological signs, predominantly ataxia and tremors.[6,14] Necropsy examination of three goats in Germany revealed enlargement of lymph nodes and visceral organs with minute white-spots in the liver and kidney. One goat had erosions and ulcerations of the esophagus, and another had bilateral corneal opacity.[6] Microscopically, goats in the published reports[6,14] had characteristic multisystemic lymphohistiocytic necrotizing vasculitis with fibrinoid necrosis, predominantly of medium-sized arteries. In the present case, neurologic signs were observed and included weakness of the hind end. Similarly, gross findings included bilateral corneal opacity, swollen lymph nodes and multiple, pinpoint, white foci in the liver, along with splenomegaly and prominent white pulp; erosions or ulcers in the alimentary tract were not observed in this goat. As in previous reports, the salient histopathologic finding was lymphohistiocytic necrotizing vasculitis, which was observed in the kidney, urinary bladder, spleen, lymph nodes, thymus, bone marrow, alimentary tract, liver and lung of this goat. Furthermore, meningoencephalitis as a result of vasculitis, marked hyperplasia of the splenic white pulp and of T-cell dependent areas of several lymph nodes were noted in this goat, which is also consistent with MCF. As with other cases, demonstration of OvHV-2 DNA by PCR in lesioned tissues, i.e. the kidney of this goat, supported the diagnosis of MCF.[6,14]

Vasculitis is rare in goats, and the lymphohistiocytic and necrotizing nature observed in MCF has been proposed to originate from a cell-mediated and cytotoxic process. MCF virus-infected CD8+ T lymphocytes have a tropism for blood vessels, where they infiltrate vascular walls and perivascular spaces. These lymphocytes express viral glycoproteins, which can in turn recruit lymphocytes and macrophages, and produce pro-inflammatory cytokines which are cytotoxic and cause injury to vascular cells.[15] This results in lymphoproliferative and necrotizing vasculitis.

The cutaneous form of MCF has been reported in one goat. That doe had multiple erythematous papules on the distal limbs that progressed to widespread erythema, localized scaling, and thinning of the hair coat, together with focal and moderate scaling and crusting of the peribuccal skin, nares and pinnae. Microscopically, granulomatous mural folliculitis was present, resembling that reported in two Sika-deer associated with a CpHV-2 infection. MCF-like cutaneous lesions, along with PCR analysis, were considered compelling evidence to associate it with an OvHV-2 infection. Sheep-associated MCF with generalized cutaneous disease, in the absence of other 'classical' features, has been reported in cattle.[5]

In the published cases discussed above and in the present case, the affected goats were kept with sheep and other goats. Data on the OvHV-2 status of the sheep and unaffected goats in the herds was not available in any of the cases.[5,6,14] However, the source of infection was tentatively attributed to contact with sheep,[5,14] as they are the recognized reservoir host for OvHV-2.[7] Although goats are the endemic carriers for CpHV-2,

OvHV-2 DNA sequences have been detected in 9% of goats in North America, suggesting that goats can also be infected asymptomatically with OvHV-2.[11] The transmission from a herd of OvHV-2-positive sheep to naïve goats has been demonstrated in a study involving a low number of animals. On the contrary, transmission from a herd of OvHV-2 infected goats did not occur during close contact with other goats over a one year period.[9]

JPC Diagnosis: Kidney: Vasculitis, lymphoblastic, necrotizing, multifocal, severe, with fibrinoid change, lymphoplasmacytic interstitial nephritis and tubular degeneration and necrosis.

Conference Comment: The contributor provides an excellent, comprehensive assessment of the epidemiology, pathogenesis and clinical presentation of malignant catarrhal fever in various species. Following a brief overview of classification schemes and general characteristics of the *Herpesviridae* family (see WSC 2013-14 conference 2, case 3), conference participants discussed two broad categories of vasculitis: infectious and non-infectious.[14] The etiologic agents of infectious vasculitis, such as bacteria (*Erysipelothrix rhusiopathiae, Salmonella* sp.), fungi (*Aspergillus* sp.), rickettsial organisms (*Ehrlicia* sp.), helminths (*Strongylus vulgaris, Dirofilaria immitis*) and viruses (African swine fever virus, Equine infectious anemia virus), directly damage vessels.[12] Non-infectious vasculitis may also be associated with infectious agents, via immune-mediated processes, or it can be secondary to toxins as in drug reactions and uremia. Causes of immune-mediated, non-infectious vasculitis include immune complex deposition associated with type III hypersensitivity reactions, cytotoxic type II hypersensitivity reactions against the endothelium, or various inflammatory mediators.[12] The cause of the vascular damage in MCF is not fully understood, but recent work suggests the possibility of direct cytotoxicity of virus infected, dysregulated cytotoxic T cells. CD8+ T-cells and MHC-unrestricted natural killer cells (large granular lymphocytes) are two of the major inflammatory cell types implicated in MCF vasculitis. Interestingly, large granular lymphocytes generally carry the highest load of viral antigen in MCF.[6,13] Additionally, in this case, there appeared to be a fibrinoid component to the vasculitis, so participants examined a PTAH stain in order to confirm the presence of fibrin. PTAH is normally used to highlight skeletal muscle cross striations; however, it can also be used to identify fibrin. Affected vessel walls from this goat multifocally stained deep purple, providing convincing evidence of fibrinoid change.

There are five clinical patterns of MCF: peracute, head and eye, alimentary, neurological, and cutaneous. Most of the clinical patterns, with the exception of the cutaneous form, are associated with lymphoproliferation and/or vasculitis with subsequent necrosis in various tissues. The head and eye forms, characterized by ocular and nasal discharge, with lesions such as petechial hemorrhages and necrosis on the muzzle and in the mouth, are the most common forms in cattle. Diarrhea occurs in both the alimentary, and occasionally in the peracute form. The cutaneous form is distinguished grossly by alopecia with erythematous papules and crusts and microscopically by granulomatous mural folliculitis. It has been reported in cattle and one goat.[5,13] Rule outs for MCF include Jembrana disease, pestivirus, orbivirus, morbillivirus, or vesicular diseases.[2,13] Jembrana disease in Bali cattle (banteng) is caused by a lentivirus. Its principal lesion is a large number of intravascular macrophages filling and surrounding small to medium pulmonary arteries and veins.[3] Pestivirus (bovine viral diarrhea, border disease), morbillivirus (rinderpest, peste-des-petits), orbivirus (bluetongue, epizootic hemorrhagic disease, Ibaraki disease), herpesvirus (infectious bovine rhinotracheitis) and vesicular stomatitides such as rhabdovirus (vesicular stomatitis) and aphthovirus (foot and mouth disease) can all cause oral/enteric ulceration in ruminants; however, they are not generally associated with lymphoid proliferation and vasculitis.[2] Due to the variability in clinical presentation as well as its similarity to other enteric and vesicular diseases, laboratory confirmation of MCF, via PCR, ELISA or indirect immunofluorescence, is essential.[13]

Contributing Institution: Department of Pathobiology and Veterinary Science
Connecticut Veterinary Medical Diagnostic Laboratory
University of Connecticut
www.patho.uconn.edu

References:

1. Ackermann M. Pathogenesis of gammaherpesvirus infections. *Vet Microbiol*. 2006;113:211-222.
2. Brown CC, Baker DC, Barker IK. The alimentary system. In: Maxie MG, ed. *Jubb, Kennedy and Palmer's Pathology of Domestic Animals*. 5th ed. Vol 2. Philadelphia, PA: Elsevier Saunders; 2007:135-137, 140-148, 152-161.
3. Budiarso IT, Rikihisa Y. Vascular lesions in lungs of Bali cattle with Jembrana disease. *Vet Pathol.* 1992;29(3):210-215.
4. Davidson AJ, Eberle R, Ehlers B, et al. The order Herpesvirales. *Arch Virol*. 2009;154:171-177.
5. Foster AP, Twomey DF, Monie OR, et al. Diagnostic exercise: generalized alopecia and mural folliculitis in a goat. *Vet Pathol*. 2010;47 (4):760-763.
6. Jacobsen B, Thies K, Von Altrock A, et al. Malignant catarrhal fever-like lesions associated with ovine herpesvirus-2 infection in three goats. *Vet Microbiol*. 2007;124:353-357.
7. King AMQ, Lefkowitz E, Adams MJ, Carstens EB, eds. *Virus Taxonomy: Ninth Report of the International Committee on Taxonomy of Viruses*. London, UK: Elsevier/Academic Press; 2011:119-120.
8. Li H, Cunha CW, Taus NS. Malignant catarrhal fever: understanding molecular diagnostics in context of epidemiology. *Int J Mol Sci*. 2011;12:6881-6893.
9. Li H, Keller J, Knowles DP, et al. Transmission of caprine herpesvirus 2 in domestic goats. *Vet Microbiol*. 2005;107:23-29.
10. Li H, O'Toole D, Kim O, et al. Malignant catarrhal fever-like disease in sheep after intranasal inoculation with ovine herpesvirus-2. *J Vet Diagn Invest*. 2005;17:171-175.
11. Li H, Keller J, Knowles DP, et al. Recognition of another member of the malignant catarrhal fever virus group: an endemic gammaherpesvirus in domestic goats. *J Gen Virol*. 2001;82:227:232.
12. Maxie MG, Robinson WF. Cardiovascular system. In: Maxie MG, ed. *Jubb, Kennedy and Palmer's Pathology of Domestic Animals*. 5th ed. Vol. 3. Philadelphia, PA: Elsevier; 2007:69-72.
13. Russell GC, Stewart JP, Haig DM. Malignant catarrhal fever: A review. *Vet J*. 2009;179(3): 324-335.
14. Twomey DF, Campbell I, Cranwell MP, et al. Multisystemic necrotising vasculitis in a pygmy goat (*Capra hircus*). *Vet Rec*. 2006;158:867-869.
15. Zachary JF. Mechanisms of microbial infections. In: Zachary JF, McGavin MD, eds. *Pathologic Basis of Veterinary Disease*. 5th ed. St Louis, Missouri: Mosby Elsevier; 2012:219.

CASE II: 10-1729 NCSU-CVM (JPC 4004353).

Signalment: 9-year-old female spayed Pomeranian dog, (*Canis familiaris*).

History: This dog presented to the North Carolina State University College of Veterinary Medicine (NCSU-CVM) Neurology service in July 2010 for further evaluation of a two-week history of a head tilt.

Gross Pathology: In the subdural region of both cerebral hemispheres, the leptomeninges appear cloudy and multifocally contain a moderate hemorrhage in the form of petechiae and ecchymoses.

There are two sharp lines of demarcation, one that is noted at the beginning of the duodenum near the termination of the pylorus, and the other line is noted near the beginning of the jejunum. That area, which encompasses the duodenum, measures 15 cm in length, is diffusely dark red to black, and on cut surface, there is diffuse serosal and mucosal hemorrhage. The jejunum, ileum, cecum, and colon contain multifocal dark red hemorrhagic areas on the serosa that measure 1.0 cm to 2.0 cm in diameter and contain a moderate amount of hemorrhagic luminal content.

Laboratory Results:

CBC: mildly decreased hemoglobin (11.7 g/dl, reference range: 12.1-20.3 g/dl) and mild thrombocytopenia (99 x 10^3/UL, reference range 170-400 x10^3/UL).

Blood smear: unremarkable.

The neurological exam findings included the following: depressed, dull mental status; right-sided head tilt and circling to the right; mild amount of pain elicited on palpation of cranial cervical region; no vestibulo-ocular response present; positional ventral strabismus OD; and anisocoria (L>R). Lesion localization was central vestibular disease (vestibular signs with altered mentation).

Tick panel, 4 DX (*Ehrlichia*, *Anaplasma*, Heartworm, Lyme), and *Cryptococcus* antibody: all negative.

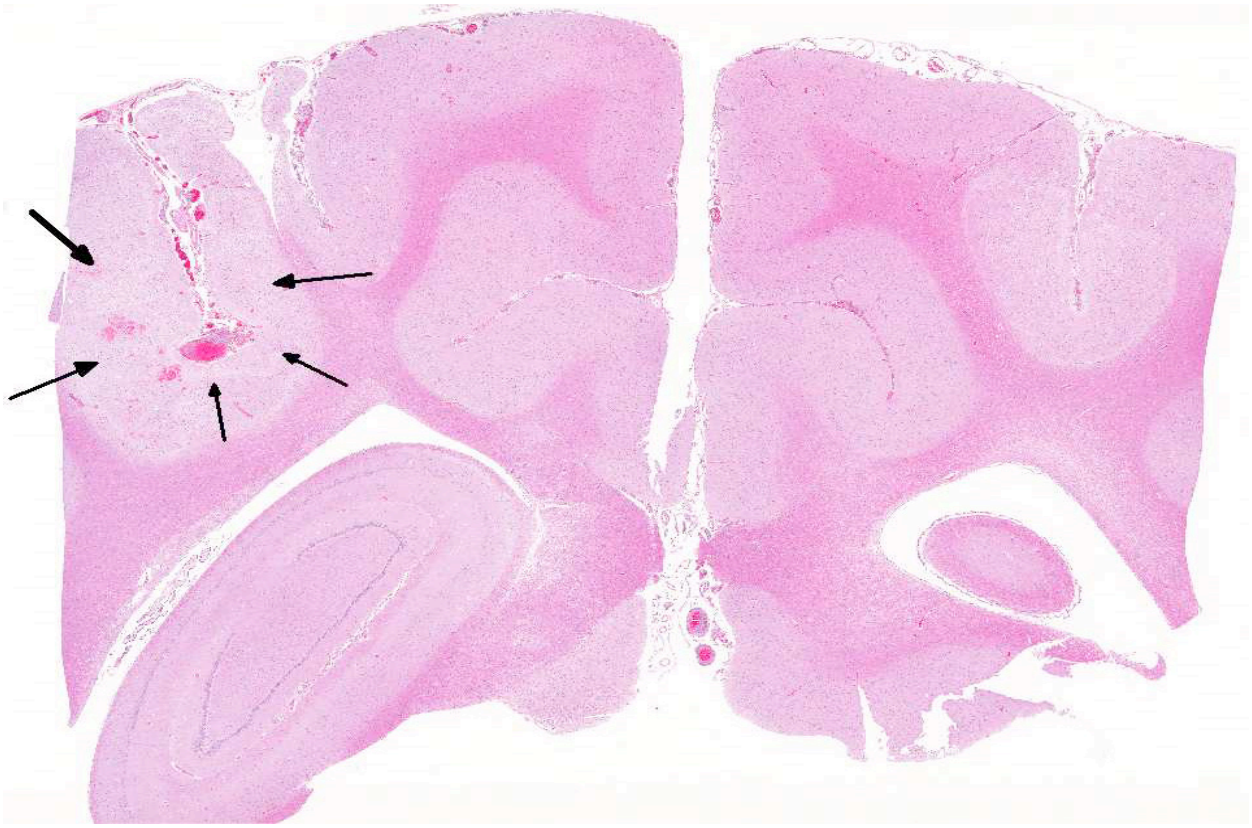

2-1. Cerebrum at level of hippocampus, dog: Meningeal vessels and vessels in the neuropil are expanded by thrombi induced by neoplastic round cells, resulting in infarction and rarefaction of the neuropil. (HE 0.63X)

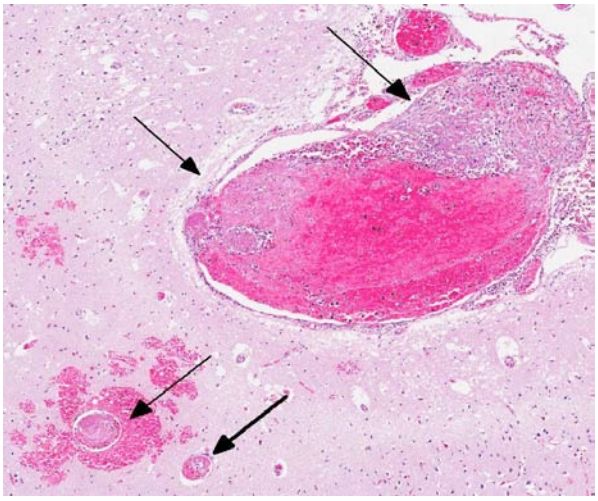

2-2. Within this area, numerous vessels contain fibrin thrombi, which are occasionally attached to vessel walls (upper left). (HE 46X)

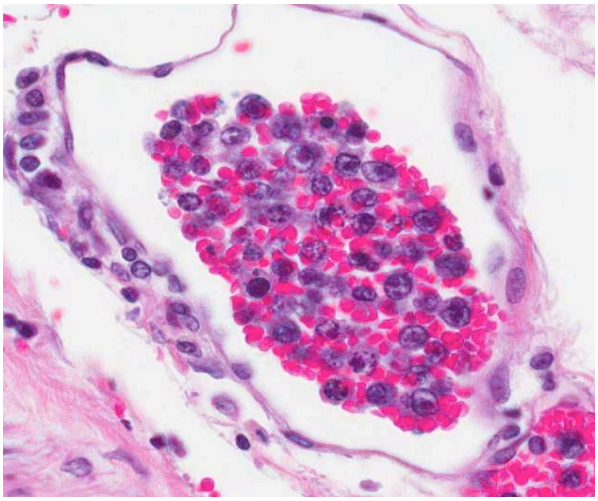

2-3. Cerebrum at level of hippocampus, dog: Neoplastic lymphocytes are present solely within vessels within the meninges and neuropil. Neoplastic cells range from 7-20 µ m, with abundant granular eosinophilic cytoplasm, irregularly round nuclei, prominent nuclei, and exhibit moderate anisocytosis and anisokaryosis. (HE 400X)

MRI: multifocal regions of parenchymal T2 hyperintensity and increased meningeal enhancement with evidence of parenchymal hemorrhage consistent with a severe meningoencephalitis, and focal regions of compensatory hydrocephalus consistent with prior parenchymal necrosis, and left otitis media.

CSF analysis: mononuclear pleocytosis (NCC 19).
Otic cytology: septic suppurative inflammation.
Otic culture: *Staphylococcus pseudintermedius.*

CD3 and CD79a immunohistochemical stains were applied to the tissue sections of cerebrum. The positive controls worked well and internal control lymphocytes were positive. CD3 immunostain revealed minimal to mild, occasional membrane staining of individual neoplastic cells within vessels. The CD79a immunostain was negative.

PARR (PCR for antigen receptor rearrangement) results for cerebrum: TCRγ PARR produced a crisp band in duplicate of the appropriate size that persisted upon heteroduplex analysis. BCR PARR was negative. PARR interpretation: These results should raise your suspicion of T cell neoplasia.

Histopathologic Description: Cerebrum: Multifocally, variably sized blood vessels within the parenchymal and meningeal layer contain neoplastic round cells. Neoplastic cells have large, round to oval nuclei, abundant coarsely clumped chromatin, sparse to moderate lightly basophilic cytoplasm, and 1-2 nucleoli. There is marked anisocytosis and ansiokaryosis and occasionally cells appear binucleated. Mitotic figures are occasionally seen. Multifocally, vessels that contain neoplastic cells also are partially occluded by fibrin thrombi that are composed of brightly eosinophilic, homogenous to beaded material and are admixed with scattered pyknotic and karyorrhectic cellular debris. Fibrin and necrotic cell debris multifocally expands and replaces the walls of scattered vessel profiles. Multifocally, expanding the meninges is a moderate cellular infiltrate that consists predominantly of lymphocytes, plasma cells, and macrophages. Multifocally, within the white matter, there are small aggregates of gitter cells. Multifocally, within the gray matter, there is a mild amount of vacuolation and a moderate amount of hemorrhage. Multifocally, admixed with the cellular infiltrate in the meninges is a moderate amount of hemosiderin laden macrophages and bright, yellow pigment consistent with hematoidin.

Additional findings (not included in slide set): The same neoplastic population of cells was seen within vascular lumens in the following organs: cervical and thoracic spinal cord, left and right bulla, liver, spleen, lung, lymph node, adrenal glands, and duodenum. Other histological findings in this animal included: moderate lymphoplasmacytic and neutrophilic cellular

Table 1: Select endothelial cell and leukocyte adhesion molecules[1]

Endothelial Molecule	Leukocyte Receptor	Major Role
P-selectin	PSGL-1 (a Sialyl-Lewis-X glycoprotein)	Rolling (neutrophils, monocytes, lymphocytes)
E-selectin	ESL-1 (a Sialyl-Lewis-X glycoprotein); Sialyl-Lewis A glycoprotein	Slow rolling, adhesion to active endothelium (neutrophils, monocytes, T-cells) Important in homing of effector & memory T-cells, especially to skin
ICAM-1	β_2-integrins: LFA-1 (CD11a/ CD18), Mac-1 (CR3; CD11b/ CD18); gp150,95 (CR4; CD11c/ CD18)	Adhesion, stable adhesion, transmigration (all leukocytes)
VCAM-1	β_1-integrins: VLA-4 ($\alpha 4\beta 1$; CD49d/CD29), LPAM-1 ($\alpha 4\beta 7$)	Adhesion (eosinophils, monocytes, lymphocytes) VLA-4 mediates homing of lymphocytes to endothelium at peripheral sites of inflammation
GlyCAM-1; MadCAM-1; CD34	L-selectin	Rolling; lymphocyte homing to high endothelial venules (HEV) Also serves to bind neutrophils to activated endothelium
PECAM (CD31)	PECAM (CD31)	Transmigration; Leukocyte migration through endothelium
CD99	CD99	Transmigration
JAM-A	JAM-A, LFA-1	Transmigration
JAM-C	JAM-B, Mac-1	Transmigration

infiltrate within the epithelium of the middle ear of the left bulla; diffuse submucosal hemorrhage in the right bulla; diffuse hemorrhagic pancreatic necrosis; transmural duodenal hemorrhage, and multifocal mucosal hemorrhage in the remainder of the intestinal tract.

Contributor's Morphologic Diagnosis: Brain with systemic organ involvement: intravascular lymphoma with multifocal vascular thrombosis.

Contributor's Comment: The histological findings and special testing in this case are most consistent with intravascular lymphoma (IVL), also known as malignant angioendotheliomatosis, intravascular lymphomatosis, and angiotropic large-cell lymphoma.[3] This neoplasm is defined by a proliferation of neoplastic lymphocytes within vessels of organs with a lack of a primary extravascular neoplasm or circulating neoplastic cells or leukemia.[3] The location of the neoplastic cells causes secondary occlusion of the vessel, which then can lead to thrombosis, hemorrhage, and infarction,[2] as in this case. In order to distinguish IVL from disseminated lymphoma and leukemia, one publication suggests that the following criteria can be used: inability to locate neoplastic cells in blood smears, lack of a primary extravascular mass, and absence of bone marrow involvement,[4] which were all consistent findings in this case. The neoplasm is predominantly of T-lymphocyte origin in dogs.[3]

Table 2: Select leukocyte integrins and extra-cellular matrix components involved in leukocyte chemotaxis[1]

Leukocyte Integrin	ECM Component
VLA-1, 2	Collagen
VLA-3, 5	Fibronectin
VLA-6	Laminin

Although this neoplasm is rare, the disease in dogs has been reported to have a predilection for CNS, lung, and less commonly skin.[3,4] One retrospective review of cases of canine IVL found that the most common clinical presentation in dogs included spinal cord ataxia, seizures, vestibular disease, and posterior paralysis.[4] The laboratory findings (CBC, chemistry panel) in the dogs in this study, as well as the dog in this case, were non-specific. Intravascular lymphoma appeared to affect mostly large breed dogs with an average age of six years.[4] The diagnosis of IVL is predominantly a postmortem diagnosis; however, there is one report of an antemortem diagnosis achieved by CT-guided biopsy of a brain lesion.[2] Intravascular lymphoma is typically rapidly progressive; death is reported to occur from 20 days to six months after the first reported clinical signs.[2]

Although the reason for the tendency of neoplastic cells to remain within vessels has not been definitively proven in dogs, several human studies have demonstrated an absence of leukocyte adhesion molecules such as CD11a/ CD18[5,7] and CD29,[6] in neoplastic cells. Based on

the findings, it was hypothesized that due to the lack of adhesion molecules, the neoplastic cells could not extravasate.

JPC Diagnosis: 1. Cerebrum: Intravascular lymphoma.
2. Midbrain, gray matter and meninges: Vascular necrosis and thrombosis, multifocal, severe with infarction.

Conference Comment: In human intravascular lymphoma, which is usually of B-cell origin, several studies have demonstrated β_1 (CD29) or β_2-integrin (CD18) deficiencies.[4,5] β-integrins are important in the leukocyte adhesion cascade, enabling leukocytes to exit blood vessels and migrate through tissue in order to participate in inflammation. Once activated, all stages of the leukocyte adhesion cascade (i.e., margination, rolling, stable adhesion, locomotion and transmigration) occur concurrently. Initial vasodilation leads to decreased hydrostatic pressure and a slowing of blood flow. Leukocytes exit laminar flow due to decreased vessel wall shear stress, and move toward the endothelial cell surface (margination). Initial rolling is mediated by selectins; low affinity binding between selectins and their receptors allows leukocytes to "roll" along the endothelium. Leukocytes in some species express L-selectin, which binds to GlyCam-1/CD34 and MadCAM-1on endothelial cells; P-selectin glycoprotein ligand-1 (PSGL-1) which is a sLe-X glycoprotein that binds to P-selectin released from endothelial Weibel-Palade bodies; and a sLe-X type protein receptor which binds E-selectin expressed by endothelial cells (Table 1). Expression of adhesion molecules is enhanced by inflammatory mediators released from mast cells, endothelial cells and macrophages in response to infection or injury. For instance, TNF and IL-1 induce endothelial cells of post-capillary venules to express E-selectin and ligands for L-selectin, while histamine, thrombin and platelet activating factor stimulate the release of P-selectin from storage within the Weibel-Palade bodies of endothelial cells.[1]

Integrins mediate stable adhesion, which must be preceded by activation, margination and rolling. Leukocytes that normally express integrins in low affinity state are activated by chemokines, while L-selectins are cleaved from the neutrophil surface by A Disintegrin and Metalloproteinase 17 (ADAM17). This results in the conversion of β_1–integrins, such as VLA-4 ($\alpha_4\beta_1$, CD49d/CD29), and β_2–integrins, such as LFA-1 (CD11a/CD18), Mac-1 (CD11b/CD18, CR3), gp150, 95 (CD11c/CD18, CR4) and $\alpha_d\beta_2$ (CD11d/CD18) to a high-affinity state. Inflammatory mediators also induce endothelial expression of ligands for β_1/β_2-integrins. These ligands generally belong to the immunoglobulin superfamily. Most β_2-integrins on appropriately stimulated leukocytes firmly adhere to ICAM-1 (CD-54) on endothelial cell; $\alpha_d\beta_2$, on the other hand, binds ICAM-3. Alternatively, β_1–integrins on lymphocytes, monocytes and high endothelial venules (HEVs) bind VCAM-1 on endothelial cells (Table 1).[1]

During transmigration, leukocytes emigrate between endothelial cells, primarily at intercellular junctions in post-capillary venules. This is mediated by adhesion molecules, which vary slightly depending on the leukocyte and tissue type. PECAM-1 (CD31) and CD99 on leukocytes bind homotypically to PECAM-1 and CD99, respectively on endothelial cells. Additionally, leukocyte junctional adhesion molecules JAM-A and JAM-B can bind to JAM-A and JAM-C at endothelial cell junctions. Leukocyte integrins also play a role in transmigration. Leukocytes extend pseudopodia between endothelial cells to interact with basement membrane laminins and collagen as well as extracellular matrix proteins such as proteoglycans, fibronectin and vitronectin. Leukocyte binding to these proteins, primarily via β_1-integrins, enables leukocytes to transmigrate into perivascular tissue, from which they can migrate along chemotactic gradients toward the area of injury. Whether endogenous (e.g., cytokines, C5a, arachidonic acid metabolites) or exogenous (e.g., bacterial) substances, chemotactic agents bind to specific G-protein coupled receptors and activate second messengers, which induces actin polymerization and allows filopodia to pull the cell into the area of inflammation. In connective tissue, leukocytes can adhere to the extracellular matrix and advance via β_1-integrins (Table 2).[1]

Deficiencies in β_1 (CD29) or β_2-integrins (CD18) have been reported in the neoplastic cells in human intravascular lymphoma. Although other defects are likely involved as well, this lack of leukocyte adhesion molecules may render

neoplastic lymphocytes unable to successfully exit the blood vessel, resulting in the intravascular cellular accumulation characteristically noted in this neoplasm. A similar leukocyte adhesion deficiency has not yet been demonstrated in canine intravascular lymphoma, and its molecular basis remains unknown.[4,5,6]

Contributing Institution: North Carolina State University, College of Veterinary Medicine, Department of Population Health and Pathobiology
http://www.cvm.ncsu.edu/ed/res_ap.html or
http://www.cvm.ncsu.edu/

References:

1. Ackermann MR. Inflammation and healing. In: Zachary JF, McGavin MD, eds. *Pathologic Basis of Veterinary Disease*. 5th ed. St. Louis, MO: Elsevier; 2012:96-98.
2. Bush WW, Throop JL, McManus PM, et al. Intravascular lymphoma involving the central and peripheral nervous systems in a dog. *J Am Anim Hosp Assoc*. 2003;39(1):90-96.
3. Ginn PE, Mansell JEKL, Rakich PM. Skin and appendages. In: Maxie, MG, ed. *Jubb, Kennedy, and Palmer's Pathology of Domestic Animals*. 5th ed. Vol. 1. Philadelphia, PA: Elsevier; 2007:775.
4. McDonough SP, Van Winkle TJ, Valentine BA, et al. Clinicopathological and immunophenotypical features of canine intravascular lymphoma (Malignant Angioendotheliomastosis). *J Comp Pathol*. 2002;126(4):277-288.
5. Ossege LM, Postler E, Pleger B, et al. Neoplastic cells in the cerebrospinal fluid in intravascular lymphomatosis. *J Neurol*. 2000;48 (8):656-658.
6. Ponzoni M, Ferreri AJM. Intravascular lymphoma: a neoplasm of "homeless" lymphocytes? *Hematol Oncol*. 2006;24(3): 105-112.
7. Valli VEO. Hematopoietic system. In: Maxie MG, ed. *Jubb, Kennedy, and Palmer's Pathology of Domestic Animals*. 5th ed. Vol. 3. Philadelphia, PA: Elsevier;2007:183.

CASE III: T11-09742 (JPC 4002867).

Signalment: 8-month-old female spayed domestic shorthair cat, (*Felis catus*).

History: An oral mass was noted when the cat yawned.

Gross Pathology: As per the clinician: the mass is "red, inflamed and appears to extend along the gumline."

Histopathologic Description: Gingiva: The tissue is composed of a mass that is characterized by fronds and islands of odontogenic epithelium that are separated by and often cradling loose or compact mesenchymal tissue. In some areas the mesenchymal tissue is forming compact round aggregates and these are the areas in which the epithelium appears to form a rim or cradle around the mesenchymal tissue. The epithelial fronds are lined by columnar cells with basal nuclei and tend to have prominent intercellular bridges. Mitotic cells are rare and primarily seen in the more compact areas of both the mesenchymal and the epithelial components. The overlying oral epithelium is segmentally ulcerated. Large numbers of neutrophils were present in the subjacent necrotic stroma and infiltrated the mesenchymal tissue of the neoplastic mass.

Contributor's Morphologic Diagnosis: Gingiva: Feline inductive odontogenic tumor (Feline inductive fibroameloblastoma).

Contributor's Comment: Feline inductive odontogenic tumor (also known as inductive fibroameloblastoma) is grouped as part of feline ameloblastic fibroma, which is characterized by epithelial and mesenchymal proliferation as a manifestation of the inductive properties of the odontogenic epithelium. Ameloblastic fibroma consists of poorly organized and more or less diffuse mesenchymal induction around the epithelial islands. A subtype of ameloblastic fibroma is the inductive fibroameloblastoma, characterized by well-formed cup-shaped epithelial structures that partially encircle stroma that resembles dental pulp.[10] The terminology "inductive" is used based on the resemblance of the epithelial islands to the cup stage of odontogenesis in which the dental lamina has an inductive effect on the stroma producing dental pulp.[6]

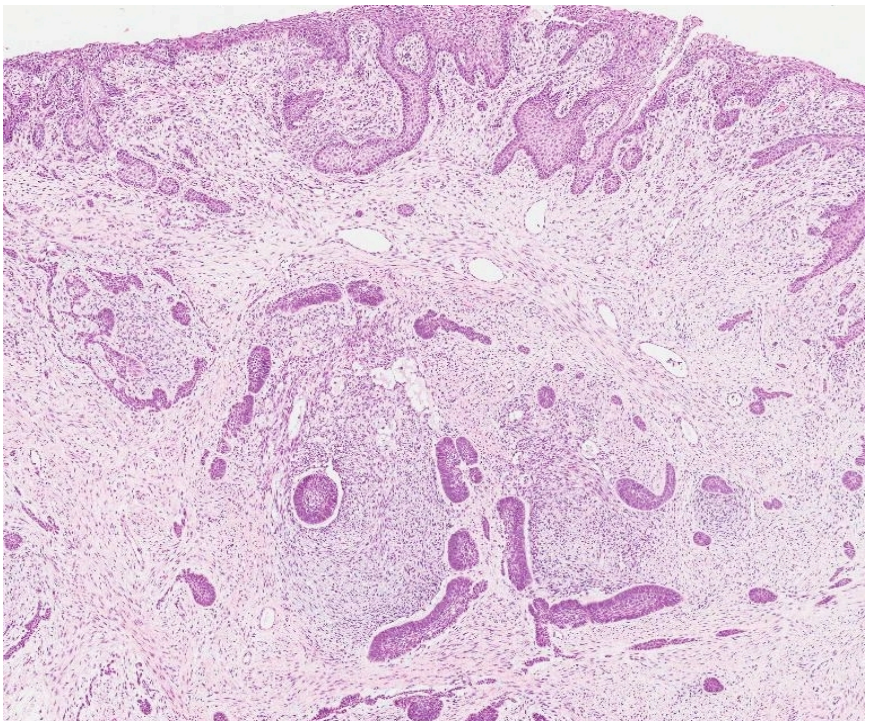

3-1. Gingiva, cat: The gingiva is expanded by an infiltrative, unencapsulated neoplasm composed of trabeculae of odontogenic epithelium and primitive mesenchyme. The overlying epithelium is ulcerated, eroded and hyperplastic. (HE 0.63X)

Feline inductive odontogenic tumors (FIOT) are rare dental tumors specific to cats.[6,7] The neoplasm is the most common dental tumor of young kittens of either sex.[10] Feline inductive odontogenic tumor is described exclusively in cats under 3 years of age[1] and is most often found on the rostral maxilla,[7,10] occasionally causing tooth loss or partial distortion. It has been confused with ameloblastoma in cats.[5] Unlike FIOT, which occurs in young cats, up to three years of age with most being younger than 18 months,[6] ameloblastomas occur in adult cats, chiefly over the age of six years and affects the maxilla and the mandible.[6]

Feline inductive odontogenic tumor is a rare and interesting

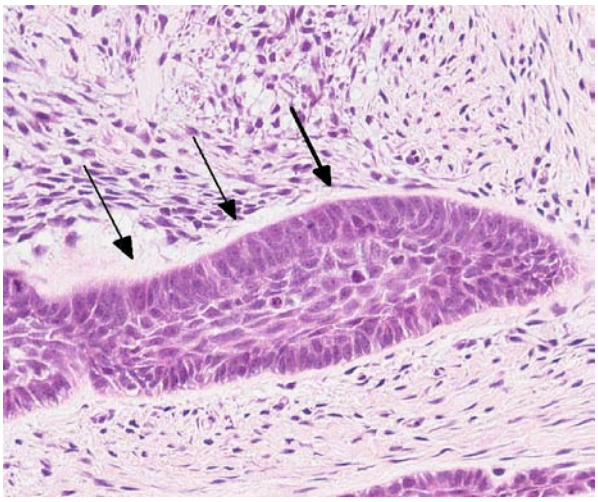

3-2. Gingiva, cat: Odontogenic epithelium is columnar, palisades along a basement membrane, and has prominent intercellular bridges. (HE 252X)

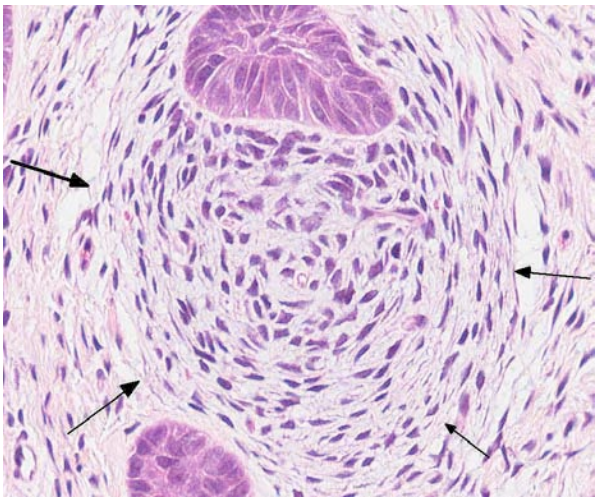

3-3. Gingiva, cat: Trabeculae of odontogenic epithelium encircle condensations of primitive mesenchyme, recapitulating dental pulp. (HE 400X)

odontogenic neoplasm in which the odontogenic epithelium has inductive potential to form aggregated foci of dental pulp-like mesenchymal cells.[9] Its biological behavior is not well elucidated. The neoplasm is thought to have a benign behavior. Some studies indicate that Type IV collagen and laminin were constantly positive around the foci of epithelial cells, and Ki-67 positive indices were extremely low. These findings are consistent with the benign clinical presentation.[9] Although, it is a benign neoplastic mass histopathologically, feline inductive odontogenic tumor grows by expansion and can infiltrate the underlying bone and cause considerable local destruction.[1] Local recurrence has been reported in incompletely excised masses; however, metastasis does not appear to occur. This tumor differs microscopically from human ameloblastic fibromas in that it is not well-circumscribed but rather originates multifocally within the supporting connective tissue as characteristic, spherical condensations of fibroblastic connective tissue (ectomesenchyme) associated with islands of odontogenic epithelium.[6]

JPC Diagnosis: Gingiva: Feline inductive odontogenic tumor.

Conference Comment: Understanding normal tooth development is helpful in understanding the various odontogenic tumors and their classifications. Teeth develop from two embryonic tissues: the buccal cavity squamous epithelium (BCSE) and the embryonic mesenchyme (EM). BCSE invaginates into the EM to become the dental lamina, which develops into the enamel organ. The enamel organ is composed of the outer enamel epithelium, inner enamel epithelium, stellate reticulum and stratum intermedium. Ameloblasts originate from the inner enamel epithelium and form a cap enclosing a nodule of mesenchyme, known as the dental papilla. Ameloblasts induce the dental papilla mesenchyme to condense at the site of the future tooth and differentiate into odontoblasts. Odontoblasts produce dentin, and dentin production re-induces ameloblasts to synthesize enamel. Dentin formation always precedes enamel formation. Odontoblasts, which initially lay down pre-dentin and then move backward toward the pulp cavity as they produce dentin, remain active throughout life, so the process of making dentin continues after eruption and the pulp cavity shrinks as the animal ages. Ameloblasts, induced by odontoblasts, differentiate as a row of palisading columnar cells facing the odontoblasts. They lay down an uncalcified matrix, and then harden it, backing away as the enamel layer is built up. In brachydonts, cementum covers dentin where it is not covered by enamel. Cementum formation over the root occurs when there is degeneration of Hertwig's epithelial root sheath allowing mesenchymal cells to come in contact with dentin. Those epithelial cells differentiate into cemtoblasts which produce cementum. In brachydonts, such as dogs and cats, once the tooth erupts through the gumline, the cells of the

stellate reticulum die and the stimulus is lost, hence the ameloblasts die and enamel can't be renewed. On the other hand, in hypsodont teeth, found in ruminants, rodents and horses, ameloblasts survive and enamel is continuously renewed. Overall, odontoblasts, dentin, cementum and pulp derive from EM (mesenchyme), while ameloblasts and enamel derive from epithelium (BCSE). The periodontal ligament, which anchors teeth into alveolar bone, is produced by ligament fibroblasts which stem from dental follicle cells.[2,3,11]

Odontogenic epithelium is characterized by 1) peripheral palisading of columnar epithelial cells, 2) apical hyperchromatic nuclei with basilar cytoplasmic clearing and 3) prominent intercellular bridging between internal epithelial cells (stellate reticulum).[2] Tumors of odontogenic epithelium are broadly divided into two categories: non-inductive tumors without odontogenic mesenchyme, including ameloblastoma, amyloid-producing odontogenic tumor and canine acanthomatous ameloblastoma, and inductive tumors with the presence odontogenic mesenchyme, including feline inductive odontogenic tumor, ameloblastic fibroma, complex odontoma and compound odontoma.[2,8,9,10]

Ameloblastoma, the least differentiated of the non-inductive odontogenic tumors, has been reported in dogs, cats, horses and humans. Ameloblastoma is classified as central (within the bone) or peripheral (within the gingival soft tissue) and is characterized by islands of poorly differentiated odontogenic epithelium, occasionally admixed with foci of metaplastic bone. Ameloblastic epithelial cells often undergo squamous differentiation and tumors are occasionally so heavily keratinized that it becomes difficult to differentiate ameloblastoma from squamous cell carcinoma. Central ameloblastomas are more common in animals.[2,8,10] The neoplastic islands of odontogenic epithelium in amyloid-producing odontogenic tumors (APOT) are separated by abundant waxy eosinophilic material (amyloid) which exhibits strong apple-green birefringence under polarized light when stained with Congo red. Recent studies have suggested the protein in APOT is not actually amyloid, but is derived from an ameoblastin-like peptide, or AAmel. Ameloblastin (formerly known as sheathlin) is an enamel matrix protein that is essential for enamel formation. Ameloblastin and another enamel protein, amelogenin, are both produced by ameloblasts during amelogenesis (see WSC 2012-13, conference 8, case 2).[2,4] Canine acanthomatous ameloblastoma is more locally aggressive than the other non-inductive odontogenic tumors and, like the ameloblastoma, is generally composed of interconnecting cords and sheets of odontogenic epithelium. It can be differentiated from ameloblastoma by an increased amount of stroma with abundant fibrillar collagen, regularly-positioned stellate mesenchymal cells, and regularly dispersed empty blood vessels, reminiscent of periodontal ligament connective tissue (see WSC 2012-13, conference 8, case 1). Cyst formation is common in acanthomatous ameloblastomas, however, in contrast to ameloblastomas, keratinization is rare.[2,8]

A comprehensive review of feline inductive odontogenic tumors is provided above by the contributor. Another inductive odontogenic tumor, ameloblastic fibroma, is composed of islands and cords of odontogenic epithelium on an abundant, collagen-poor fibrous stroma resembling dental pulp (see WSC 2011-12, conference 1, case 4). This is the most common odontogenic tumor in cattle, but has also been reported in young horses and dogs.[2,7] Complex/compound odontomas, the most differentiated odontogenic tumors, are composed of tooth-like structures known as denticles. Denticles contain enamel, dentin, cementum and pulp, arranged in a manner similar to a normal tooth; discrete islands of odontogenic epithelium are not present. These are reported in dogs, horses and cattle and can disrupt surrounding, normal teeth.[2]

Contributing Institution: The University of Georgia
Veterinary Diagnostic and Investigational Laboratory
Tifton, GA 31793
http://www.vet.uga.edu/dlab/tifton/index.php

References:

1. Beatty JA, Charles JA, Malik R, France MP, Hunt GB. Feline inductive odontogenic tumour in a Burmese cat. *Aust Vet J*. 200;78(7):452-455.
2. Brown CC, Baker DC, Barker IK. The alimentary system. In: Maxie MG, ed. *Jubb, Kennedy and Palmer's Pathology of Domestic Animals*, 5th ed. Vol 2. Philadelphia, PA: Elsevier

Saunders; 2007:5-7, 24-28.
3. Caceci T. Digestive System I: Oral Cavity & Associated Structures. VM8054: Veterinary Histology website. http://www.vetmed.vt.edu/education/Curriculum/VM8054/Labs/labtoc.htm. Accessed October 29, 2013.
4. Delaney MA, Singh K, Murphy CL, Solomon A, Nel S, Boy SC. Immunohistochemical and biochemical evidence of ameloblastic origin of feline amyloid-producing odontogenic tumors in cats. *Vet Pathol*. 2013;50(2):238-242.
5. Gardner DG. Ameloblastomas in cats: a critical evaluation of the literature and the addition of one example. *J Oral Pathol Med*. 1998;27(1):39-42.
6. Gardner DG, Dubielzig RR. Feline inductive odontogenic tumor (inductive fibroameloblastoma) – a tumor unique to cats. *Journal of Oral Pathology & Medicine*. 1995;24:185–190.
7. Head KW, Else RW, Dubielzig RR. Tumors of the alimentary tract. In Meuten DJ, ed. *Tumors in Domestic Animals*. 4th ed. Ames, IA: Iowa State Press; 2002:401-481.
8. Head KW, et al. Tumors of odontogenic epithelium without odontogenic mesenchyme. In: *Tumors of the Alimentary System of Domestic Animals*. Washington DC: AFIP and CL Davis DVM Foundation and WHO Collaborating Center for Worldwide Reference on Comparative Oncology; 2003:49-51.
9. Hiroki Sakai, Takashi Mori, Tsuneyoshi Iida, Yanai Tokuma, Kouji Maruo and Toshiaki Masegi. Immunohistochemical features of proliferative marker and basement membrane components of two feline inductive odontogenic tumours. *Journal of Feline Medicine & Surgery.* 2008;10(3):296-299.
10. Poulet FM, Valentine BA, Summers BA. A Survey of epithelial odontogenic tumors and cysts in dogs and cats. *Vet Pathol*. 1992;29:369-380.
11. Tutt C. Tooth development (odontogenesis). In: *Small Animal Dentistry: A Manual of Techniques*. 2006:1-32.

CASE IV: 11-0193-1/2 (4035415).

Signalment: Adult male rhesus macaque, (*Macaca mulatta*).

History: This animal was euthanized for research purposes.

Gross Pathology: Postmortem examination revealed an adult male rhesus macaque in good body condition with excess subcutaneous and mesenteric adipose stores. The liver was markedly enlarged, friable, and mottled dark brown, olive, and pale yellow. Sections of liver were submitted in 10% neutral buffered formalin and post-fixed in 2.5% glutaraldehyde for transmission electron microscopy.

Electron Microscopic Description:

11-0193-1:

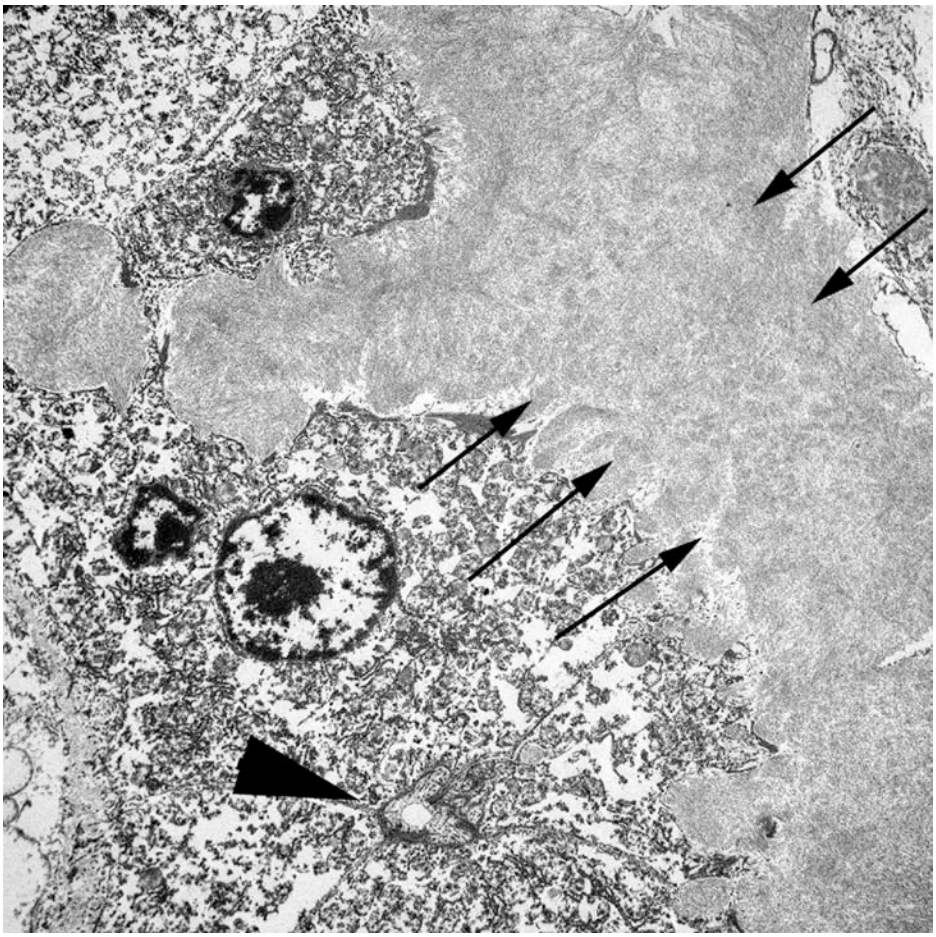

4-1. Liver, rhesus macaque: Several compressed (atrophic) hepatocytes surround a bile canaliculus (arrowhead) and are separated and surrounded by a loosely and haphazardly arranged fibrillar material amyloid. (Photo courtesy of: Integrated Research Facility, Division of Clinical Research, NIAID, NIH, 8200 Research Plaza, Fort Detrick, Frederick, MD 21702, Srikanth.yellayi@nih.gov). (Electron Microscopy)

This electron micrograph contains portions of 5 large polygonal cells, 4 of which converge to form a 2 µm diameter channel lined by a microvillous brush border (bile canaliculus). The cell in the center of the image is 22 µ m in greatest dimension and contains abundant, medium-electron dense, bland cytoplasm, and 2 round nuclei with prominent nucleoli and peripherally condensed heterochromatin (binucleate hepatocyte). The cells are bordered by a 15 µm wide branching sinusoid which is filled with large numbers of densely packed, pale, randomly-oriented and interlacing, non-branching, ~10nm diameter fibrils (amyloid).

11-0193-2:

This electron micrograph contains 2 distinct types of extracellular fibrillar material. Centrally there is a 3 µm wide bundle of ~50nm diameter, banded fibrils arranged in regular parallel arrays (collagen). Above and below the collagen bundle, there are large numbers of densely packed, medium-electron dense, randomly-oriented and interlacing, non-branching, ~10nm diameter fibrils (amyloid). A small portion of a cell is visible at the bottom of the image.

Contributor's Morphologic Diagnosis: Liver: Amyloidosis, sinusoidal, with focal fibrosis.

Contributor's Comment: Amyloid is an extracellular proteinaceous material composed of approximately 95% fibrillar proteins, and 5% amyloid P protein, proteoglycans, and glycosaminoglycans.[12] Conformationally, the

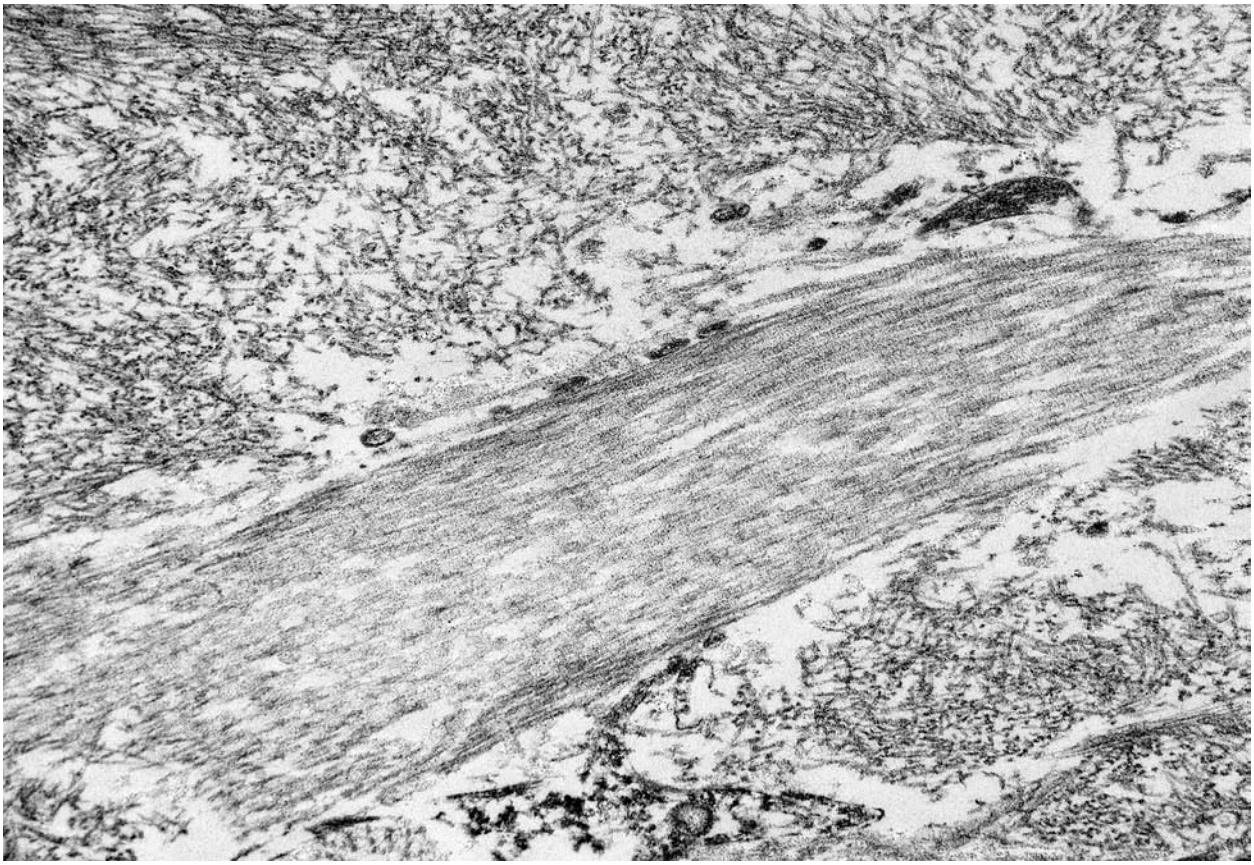

4-2. Liver, rhesus macaque: A 3 µm wide bundle of collagen (arranged in parallel and with an obvious periodicity – center) divides the loosely and haphazardly arranged amyloid fibrils (upper left and bottom right). (Photo courtesy of: Integrated Research Facility, Division of Clinical Research, NIAID, NIH, 8200 Research Plaza, Fort Detrick, Frederick, MD 21702, Srikanth.yellayi@nih.gov). (Electron Microscopy)

fibrils form regular arrays of β-pleated sheets which allows for positive Congo Red staining and a characteristic green birefringence when viewed under polarized light.[12] Numerous biochemical forms of amyloid have been identified. The amyloid light chain (AL) form is composed of intact or fragmented immunoglobulin light chains, and is associated with immune cell dyscrasias (primary amyloidosis).[12] The amyloid-associated (AA) form is derived from the acute phase protein, serum amyloid A, and is associated with chronic inflammation (secondary amyloidosis).[12] Other commonly recognized types include Aβ amyloid and islet amyloid, which are associated with cerebral amyloid angiopathy of Alzheimer's disease, and Type II diabetes mellitus, respectively.[15,16]

Amyloidosis is the pathologic accumulation of amyloid in tissues and can be systemic or localized. It has been identified in mammals, reptiles, and birds and is a well-recognized condition in rhesus monkeys and other macaques.[1,7,8,17]

By light microscopy, amyloid has a homogenous eosinophilic hyaline appearance which can be similar to other extracellular fibrillar proteinaceous deposits, such as collagen or fibrin. Ultrastructurally, however, it has a distinct appearance and can be readily differentiated, as seen in this case. When viewed with transmission electron microscopy, amyloid fibrils are non-branching, 7.5-10nm in diameter, and randomly-oriented and interlacing.[3] This is in contrast to collagen which has larger fibrils (~50nm in diameter) that are banded and arranged in regular parallel arrays; and fibrin, the strands of which vary in diameter and form dense irregularly-branching mats, generally in the vicinity of platelets.[4,5]

JPC Diagnosis: Liver, space of Disse: Amyloidosis with hepatocellular compression.

Conference Comment: Amyloidogenic proteins have a tendency toward misfolding which leads to the formation of unstable, self-associated fibrils.[12] Reactive systemic (secondary) amyloidosis is the

most common form of amyloidosis in domestic animals. Tissue accumulations is caused by overproduction of AA amyloid, in combination with reduced destruction, and is often associated with chronic inflammatory or neoplastic diseases.[7,9] The precursor to AA, serum amyloid A (SAA), is an acute phase protein produced by the liver during inflammatory conditions under the influence of IL-6 and IL-1. SAA is normally degraded by the monocyte-macrophage system,[12,13] however, a prolonged increase in SAA alone is not sufficient to induce amyloidosis. Several explanations for the development of reactive amyloidosis have been proposed, including a defective SAA degradation system and an inherent alteration in quality of SAA, which renders it resistant to complete degradation.[12]

Systemic AA amyloidosis can also be inherited in humans (familial Mediterranean fever), Chinese Shar-Pei dogs (autosomal recessive Familial AA amyloidosis), Abyssinians (autosomal dominant with incomplete penetrance) and Siamese cats. In Shar-Peis with inherited amyloidosis, amyloid is preferentially deposited in the renal medullary interstitium, while in Abyssinian cats, deposition is glomerular and in Siamese cats amyloid deposits accumulate in the hepatic space of Disse. Whether reactive or inherited, clinical signs in systemic amyloidosis are generally secondary to dysfunction of adjacent organs and pressure atrophy in areas adjacent to amyloid accumulation.[12,13]

In dogs, AA amyloidosis is usually idiopathic, but it has also been associated with *Hepatozoon americanum*, *Ehrlichia canis* and other causes of chronic suppurative/granulomatous inflammation. Canine AA amyloidosis lesions usually occur within renal glomeruli, which leads to proteinuria and progressive renal insufficiency.[13] In contrast, feline amyloidosis primarily affects the renal medulla, so proteinuria is not a typical clinical finding.[13] Equine systemic AA amyloidosis is a well-recognized hepatic lesion in horses used to produce hyperimmune serum.[13] Glomerular amyloidosis, with accompanying proteinuria, occurs occasionally in ruminants. Swine rarely develop amyloidosis.[13] Much like the other forms of reactive amyloidosis described above, avian amyloidosis tends to develop after a period of chronic inflammation and occurs most frequently in waterfowl, although it has also been reported in chickens (amyloid arthropathy).[9] Conversely, reactive amyloidosis is rarely reported in reptiles (snakes and tortoises).[17]

Reactive amyloidosis has been described in the Patas monkey, squirrel monkey, mandrill, chimpanzee, barbary ape and cynomolgus and rhesus macaques; incidence generally increases with age, likely due to cumulative exposure to parasites, infectious agents and injury.[7] Non-human primates with reactive amyloidosis often have concurrent arthritis and/or enterocolitis. Deposition typically occurs in the large or small intestine, or less commonly in the spleen, lymph node, liver, adrenal glands or stomach.[1,7] Affected animals often display elevated levels of alkaline phosphatase, aspartate aminotransferase, lactate dehydrogenase and serum amyloid A, in combination with decreased albumin and cholesterol on serum chemistry profiles.[8] Additionally, the cynomolgus macaque, rhesus macaque, squirrel monkey, gray mouse lemur and common marmoset have all been used as models for cerebral amyloidosis.[7]

Amyloidosis is a common age related change in laboratory mice, especially in CD-1 strains.[14] Mouse amyloidosis is typically composed of AA amyloid or AapoAII (senile amyloid) deposits, but mice are also subject to several localized forms of amyloidosis involving the brain or endocrine tumors. In contrast to AA amyloid, AapoAII deposition is less marked in the liver and spleen, with more deposition in adrenals, intestine, heart, lungs, thyroid and gonads. CBA and B6 mice are most susceptible to reactive (AA) amyloidosis, while A/J mice are resistant, and A/J and SJL mice are predisposed to AapoAII amyloidosis.[11] In hamsters, as in many other species, the incidence of amyloidosis increases with age. Interestingly, females are three times more likely to develop amyloidosis than males, likely due to a "hamster female protein," which is similar to amyloid P. The liver, kidneys and adrenal glands are the most frequently involved organs.[11] Amyloidosis in gerbils has been experimentally associated with filariid infection, but it also occurs spontaneously in older animals. Similarly, renal amyloidosis is reported in aged rabbits, especially those that have been hyperimmunized for antibody production.[11]

As noted by the contributor, primary amyloidosis with AL amyloid is often associated with immune cell dyscrasias. Cutaneous amyloidosis occurs in

approximately 10% of dogs and cats with extramedullary plasmactyomoas. Cutaneous amyloidosis in dogs is also associated with dermatomyositis and monoclonal gammopathy. In horses, the cause of nodular AL amyloid deposition within the skin and upper respiratory tract is unknown.[6]

In addition to AA, AL and Aβ amyloid discussed above, islet amyloid is significant in several veterinary species. Islet amyloid polypeptide (IAPP) produced by pancreatic islet β-cells in some species of mammals, birds and fishes. Although the exact pathogenesis is still unknown, IAPP can be deposited in pancreatic islets as amyloid in cats, non-human primates and humans, resulting in type 2 diabetes.[16] Endocrine disorders of the pancreas have been associated with amyloid deposits in the cynomolgus macaqe,[10] rhesus macaqe,[5] baboon, Celebes crested macaque, and Formosan rock macaque.[7]

Contributing Institution: Integrated Research Facility
Division of Clinical Research, NIAID, NIH
8200 Research Plaza
Fort Detrick
Frederick, MD 21702

References:

1. Blanchard JL, Baskin GB, Watson EA. Generalized amyloidosis in rhesus monkeys. *Vet Pathol*. 1986;23(4):425-430.
2. Cheville NF. Extracellular substances, pigments, and crystals. In: Cheville NF, ed. *Ultrastructural Pathology: An Introduction to Interpretation*. Ames, Iowa: Iowa State University Press; 1994:304-308.
3. Cheville NF. Extracellular Substances, Pigments, and Crystals. In: Cheville NF, ed. *Ultrastructural Pathology: An Introduction to Interpretation*. Ames, Iowa: Iowa State University Press; 1994:279.
4. Cheville NF. Blood and hemostasis. In: Cheville NF, ed. *Ultrastructural Pathology: An Introduction to Interpretation*. Ames, Iowa: Iowa State University Press; 1994:407.
5. De Koning EJ, Bodkin NL, Hansen BC, Clark A. Diabetes mellitus in *Macaca mulatta* monkeys is characterised by islet amyloidosis and reduction in beta-cell population. *Diabetologia*. 1993;36(5): 378-384.
6. Ginn PE, Mansell JEKL, Rakich PM. Skin and appendages. In: Maxie MG, ed. *Jubb, Kennedy, and Palmer's Pathology of Domestic Animals*. 5th ed. Vol. 1. Philadelphia, PA: Elsevier; 2007:662, 776.
7. Hukkanen RR, Liggitt HD, Anderson DM, et al. Detection of systemic amyloidosis in the pig-tailed macaque (*Macaca nemestrima*). *Comp Med*. 2006;56(2):119-27.
8. MacGuire JG, Christe KL, Yee JL, et al. Serologic evaluation of clinical and subclinical secondary hepatic amyloidosis in rhesus macaque (*Macaca mulatta*). *Comp Med*. 2009;59(2): 168-73.
9. Murakami T, Inoshima Y, Sakamoto E, et al. AA amyloidosis in vaccinated growing chickens. *J Comp Pathol*. 2013;149(2-3);291-297.
10. O'Brien TD, Wagner JD, Litwak KN, et al. Islet amyloid and islet amyloid polypeptide in cynomolgus macaques *(Macaca fascicularis):* An animal model of human non-insulin-dependent diabetes mellitus. *Vet Pathol*. 1996;33(5):479-485.
11. Percy DH, Barthold SW, eds. *Pathology of Laboratory Rodents and Rabbits*. 3rd ed. Ames, IA: Blackwell Publishing; 2007:93-94, 200-201, 301.
12. Snyder PW. Diseases of immunity. In: McGavin MD, Zachary JF, eds. *Pathologic Basis of Veterinary Disease*. 5th ed. St. Louis, Missouri: Mosby Elsevier; 20012:37-38, 284-288.
13. Stalker MJ, Hayes MA. Liver and biliary system. In: Maxie MG, ed. *Jubb, Kennedy and Palmer's Pathology of Domestic Animals*, 5th ed. Vol 2. Philadelphia, PA: Elsevier Saunders; 2007:315-316, 463-464, 532.
14. Thoolen B, Maronpot RR, Harada T, et al. Proliferative and nonproliferative lesions of the rat and mouse hepatobiliary system. *Toxicol Pathol*. 2010;38(7 suppl):5S-81S.
15. Uno H, Alsum PB, Dong S, et al. Cerebral amyloid angiopathy and plaques, and visceral amyloidosis in aged macaques. *Neurobiol Aging*. 1996;17(2):275-281.
16. Westermark P, Andersson A, Westermark GT. Islet amyloid polypeptide, islet amyloid, and diabetes mellitus. *Physiol Rev*. 2011;91(3): 795-826.
17. Zschiesche W, Jakob W. Pathology of animal amyloidoses. *Pharmac Ther*. 1989;41(1-2):49-83.